Journal of Alzheimer's Disease 52 (2016) 913–927
DOI 10.3233/JAD-160008
IOS Press

Longitudinal Study of Impaired Intra- and Inter-Network Brain Connectivity in Subjects at High Risk for Alzheimer's Disease

Yafeng Zhan[a,b], Jianhua Ma[a,*], Aaron F. Alexander-Bloch[c], Kaibin Xu[b,d], Yue Cui[b,d], Qianjin Feng[a], Tianzi Jiang[b,d,e,f] and Yong Liu[b,d,*] for the Alzheimer's Disease Neuroimaging Initiative[1]
[a]*School of Biomedical Engineering, Southern Medical University, Guangzhou, China*
[b]*Brainnetome Center, Institute of Automation, Chinese Academy of Sciences, Beijing, China*
[c]*Department of Psychiatry, Yale University School of Medicine, New Haven, CT, USA*
[d]*National Laboratory of Pattern Recognition, Institute of Automation, Chinese Academy of Sciences, Beijing, China*
[e]*CAS Center for Excellence in Brain Science, Institute of Automation, Chinese Academy of Sciences, Beijing, China*
[f]*Queensland Brain Institute, University of Queensland, Brisbane, Australia*

Handling Associate Editor: Jun-Tai Yu

Accepted 17 February 2016

Abstract. Alzheimer's disease (AD) is associated with abnormal resting-state network (RSN) architecture of the default mode network (DMN), the dorsal attention network (DAN), the executive control network (CON), the salience network (SAL), and the sensory-motor network (SMN). However, little is known about the disrupted intra- and inter-network architecture in mild cognitive impairment (MCI). Here, we employed *a priori* defined regions of interest to investigate the intra- and inter-network functional connectivity profiles of these RSNs in longitudinal participants, including normal controls ($n = 23$), participants with early MCI ($n = 26$), and participants with late MCI ($n = 19$). We found longitudinal alterations of functional connectivity within the DMN, where they were correlated with variation in cognitive ability. The SAL as well as the interaction between the DMN and the SAL were disrupted in MCI. Furthermore, our results demonstrate that longitudinal alterations of functional connectivity are more profound in earlier stages as opposed to later stages of the disease. The increased severity of cognitive impairment is associated with increasingly altered RSN connectivity patterns, suggesting that disruptions in functional connectivity may contribute to cognitive dysfunction and may represent a potential biomarker of impaired cognitive ability in MCI. Earlier prevention and treatment may help to delay disease progression to AD.

Keywords: Default mode network, early mild cognitive impairment, late mild cognitive impairment, resting-state network, salience network

[1]Data used in preparation of this article were obtained from the Alzheimer's Disease Neuroimaging Initiative (ADNI) database (http://adni.loni.usc.edu). As such, the investigators within the ADNI contributed to the design and implementation of ADNI and/or provided data but did not participate in analysis or writing of this report. A complete listing of ADNI investigators can be found at: http://adni.loni.usc.edu/wp-content/uploads/how_to_apply/ADNI_Acknowledgement_List.pdf

*Correspondence to: Yong Liu, PhD, Brainnetome Center, Institute of Automation, Chinese Academy of Sciences, Beijing 100190, China. E-mail: yliu@nlpr.ia.ac.cn and Jianhua Ma, PhD, School of Biomedical Engineering, Southern Medical University, Guangzhou 510515, China. E-mail: jhma@smu.edu.cn.

INTRODUCTION

Alzheimer's disease (AD) is the most common neurodegenerative disorder, with symptoms typically including executive dysfunction, cognitive decline, and language deficits [1–3]. Mild cognitive impairment (MCI) is a transitional state between healthy aging and the dementia that eventually occurs in AD [4, 5]. The prodromal phase of AD before dementia may last for a decade or more. Therefore, MCI has received extensive investigative attention because of the high risk of converting to AD (annual conversion rate 10–15% in MCI, compared to 1–2% in the healthy elderly population) [6–9]. To define an incipient stage for disease detection, the Alzheimer's Disease Neuroimaging Initiative (ADNI, ADNI GO and ADNI 2) has sub-classified MCI into early MCI (EMCI) and late MCI (LMCI). EMCI refers to performance between 1.0 and 1.5 standard deviations (SD) below the normative mean on a standard memory test, while LMCI refers to performance more than 1.5 SD below the normative mean on the same test [10, 11].

Resting-state functional magnetic resonance imaging (rs-fMRI) has been increasingly used to explore brain function by measuring correlations between spontaneous blood oxygen level-dependent (BOLD) signal of topographically-separated regions during "rest" (absence of task), since the first study by Biswal and colleagues [12]. Correlated spatially-distributed brain regions have been classified into several resting-state networks (RSNs), which reflect functional integration and segregation of brain activity [13, 14]. Convergent evidence suggests that the default mode network (DMN), the executive control network (CON), the salience network (SAL), the dorsal attention network (DAN), and the sensory-motor network (SMN) are among the most reproducible RSNs [15–19]. These RSNs not only reflect human brain structure and function but also provide potential clinical value as sensitive markers of disease processes [20–22].

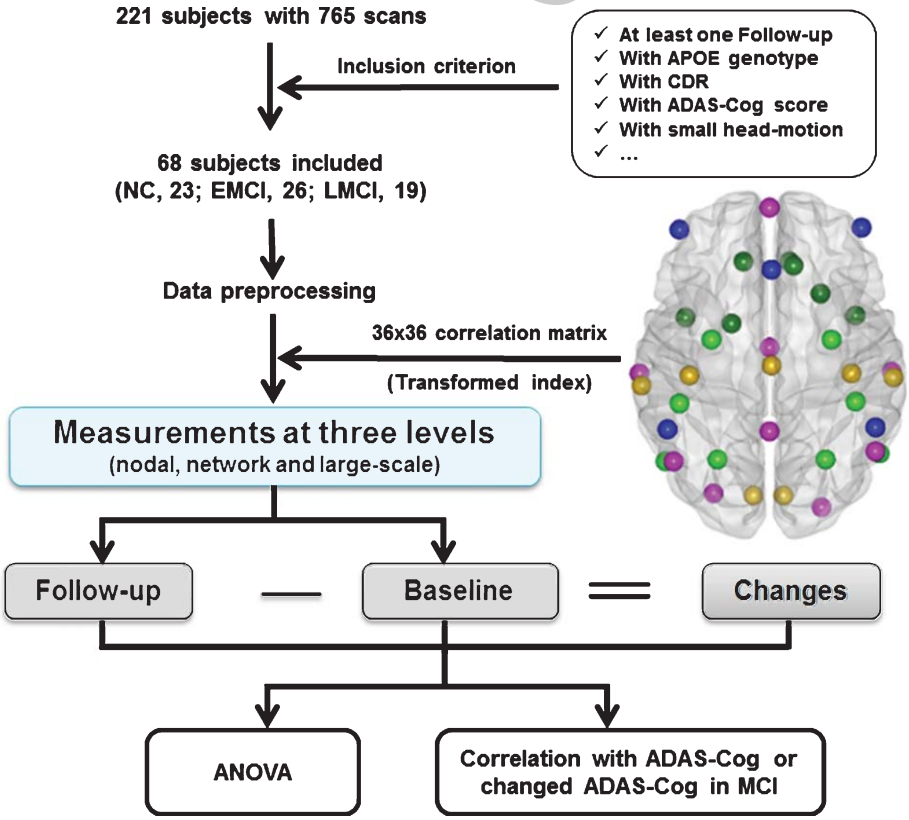

Fig. 1. Schematic of data analysis pipeline. Regional mean fMRI time series were extracted for each ROI per subject who met inclusion criteria. Correlations between each ROI pair among 36 ROIs were calculated for baseline and follow-up visits. Longitudinal changes were obtained by subtracting baseline from the follow up scan. One-way ANOVA was performed on all three groups (normal control, EMCI, and LMCI) at three levels of analysis (nodal integration, RSN profile, and large-scale connectivity). Correlations between metrics and ADAS-Cog were estimated among EMCI and LMCI.

Many studies have reported functional abnormalities and structural atrophy of DMN, in support of the hypothesis that this RSN is preferentially affected by AD [21, 23–25] and MCI [17, 26, 27]. Previous longitudinal studies of MCI and AD revealed longitudinal functional connectivity patterns of DMN deficits using independent component analysis (ICA) [28, 29]. In addition, DAN, associated with top-down attentional processing and externally-directed cognition [30], was reported to exhibit reduced functional connectivity in patients with MCI [17, 31]. A recent study revealed that AD pathology is present in sensory- and motor-related regions such as auditory and visual association cortex and motor pathways [32]. More importantly, the human brain may support information integration across spatially segregated brain regions (interactions between RSNs) in a manner that confers resilience against pathological attack [33, 34]. Several studies indicate that dysfunction of core networks of the brain such as DMN, CON, and SAL results in abnormalities in other networks with which these core networks interact [35–37]. Therefore, studying the organization of intra- and inter-network connectivity in the context of cognitive changes observed in individuals at high risk for AD may shed light on the neurological basis of cognitive decline in AD [17, 38].

The sub-classification into early and late MCI provides an opportunity to investigate alterations related to disease severity in early stages of the disease. We hypothesized that both intra-network functional connectivity and the interactions between RSNs would be impaired in MCI compared to the normal control (NC) group. We also hypothesized that longitudinal alterations in brain functional connectivity would covary with the severity of cognitive impairment. To test these hypotheses, we performed a region of interest (ROI) correlation analysis on a large, clinically-graded longitude sample. We constructed connected brain networks for 23 NC subjects, 26 patients with EMCI, and 19 patients with LMCI using *a priori* defined brain regions representing the five core RSNs [38]. We tested for disease-related alterations in functional connectivity with three different levels of analysis: 'nodal integration' (each node's connectivity with the rest of the nodes); 'RSN profile' (intra- and inter-network connectivity patterns for each network); and 'large-scale connectivity' (pairwise connectivity between every ROI). We also tested for continuous relationships between brain network measurements and cognitive ability (Fig. 1).

MATERIALS AND METHODS

Standard protocol approvals, registrations, and patient consents

The dataset used in the current study was obtained from the ADNI database (http://adni.loni.usc.edu/). According to ADNI protocol, written consent was obtained from all subjects participating in the study, and the study was approved by the institutional review board at each participating site.

Subjects

Participants were recruited through ADNI GO and ADNI 2 from over 50 centers in the USA and Canada. This study utilized ADNI data through June 2014, comprising a total of 221 participants with 765 scans. Individuals in the present study were classified as subjects with NC, EMCI and LMCI according to clinical and behavioral measures provided by ADNI GO and ADNI 2 (http://adni.loni.usc.edu/). ADNI was launched in 2003 as a public-private partnership, led by Principal Investigator Michael W. Weiner, MD. The primary goal of ADNI has been to test whether serial magnetic resonance imaging (MRI), positron emission tomography (PET), clinical measures, neuropsychological assessments and other biological markers can be combined to measure the progression of MCI and AD.

The present study included 68 participants: 23 NC subjects (12 males, mean age 74.0 ± 5.4 years at first scan, mean interval between scans 6.5 ± 1.9 months); 26 patients with EMCI (10 males, mean age at first scan 71.2 ± 7.9 years, mean scan interval 6.2 ± 1.3 months); and 19 patients with LMCI (13 males, mean age at first scan 73.2 ± 8.5, mean scan interval 7.2 ± 2.5 months). Each subject underwent a battery of neuropsychological tests and functional tests, including the Alzheimer's Disease Assessment Scale (ADAS), the Clinical Dementia Rating Scale (CDR), the Mini-Mental State Examination (MMSE), and the Functional Activities Questionnaires (FAQ). Details can be found http://adni.loni.usc.edu/methods/documents/. Demographic, psychological characteristics and statistics related to data preprocessing are summarized in Table 1.

The inclusion criteria were as follows: 1) at least two visits during the time of study; 2) CDR of 0 and MMSE scores of 26 or higher for the NC group; 3) CDR of 0.5 and MMSE scores of 24 or higher for the MCI group; 4) no change in categorical disease

Table 1
Demographics of participants

	NC (23)	EMCI (26)[a]	LMCI (19)	*p* value
Gender (M/F)	12/11	10/16	13/6	0.139
CDR	0	0.5	0.5	—
APOE (4/non 4)	8/15	12/14	7/12	—
Baseline				
Age (year)	74.0 (5.4)	71.2 (7.9)	73.2 (8.5)	0.400
MMSE	29.2 (1.0)	28.3 (1.2)	27.6 (1.2)	0.002*
ADAS-Cog	7.7 (4.3)	11.6 (6.1)	17.4 (6.5)	0.000*
Head Motion	0.6 (0.4)	0.7 (0.4)	0.6 (0.3)	0.800
Follow-up				
Age (year)	74.5 (5.4)	71.7 (7.9)	73.8 (8.6)	0.392
MMSE	29.3 (1.0)	28.1 (1.6)	27.7 (1.8)	0.003*
ADAS-Cog	7.6 (4.0)	12.6 (6.6)	16.6 (6.7)	0.000*
Head Motion	0.6 (0.4)	0.7 (0.4)	0.8 (0.6)	0.281
Changes				
Duration (month)	6.5 (1.9)	6.2 (1.3)	7.2 (2.5)	0.199
Changed MMSE	0.1 (1.4)	–0.2 (1.3)	0.1 (1.9)	0.689
Changed ADAS-Cog	–0.04 (3.5)	1.0 (4.4)	–0.8 (4.2)	0.685

Note: Values are mean ± SD. Chi-squared tests were used for gender comparisons; one-way ANOVA and *post hoc t* tests were used for age, MMSE and ADAS-Cog comparisons. MMSE, Mini-Mental State Examination; ADAS-Cog, Alzheimer's Disease Assessment Scale; CDR, Clinical Dementia Rating; APOE, Apolipoprotein E $\varepsilon 4$ allele. *Indicates a statistical difference between groups, $p < 0.05$. [a]One of follow-up of EMCI CDR is 0.

status at the follow-up visit. Additionally, because apolipoprotein E (APOE) $\varepsilon 4$ allele is associated with an increased risk for AD and many studies have revealed that the APOE $\varepsilon 4$ allele has potential effects on brain activity [20] and functional connectivity [39], we only included subjects with APOE genotype information in order to correct for the genotype effect on functional connectivity. The following exclusion criteria were applied: 1) obvious distortion on the raw imaging files; 2) translation or rotation in any axis of head motion larger than the size of one voxel during the scanning. For full ADNI inclusion/exclusion criteria, see http://www.adni-info.org.

Data acquisition

According to ADNI protocol (http://adni.loni.usc.edu/), the resting-state fMRI data was acquired on 3.0 Tesla Philips scanners (varied models/systems) while subjects were instructed to keep their eyes open. Images were acquired using an echo planar imaging (EPI) sequence with a repetition time (TR) ranging from 2250 ms to 3090 ms; echo time (TE) = 30 ms; flip angle (FA) = 80; slices = 48; field of view (FOV) = 212 mm RL, 198.75 mm AP, 159 mm FH. The imaging resolution in the X and Y dimensions ranged from 2.29 mm to 3.31 mm, and the slice thickness was 3.3 mm. For each subject, 140 volumes were acquired with a total scan duration of 420 seconds. Some individuals received extended scans with 200 volumes for a total duration of 600 seconds. For consistency, only the first 140 volumes of these scans were analyzed.

Data preprocessing

The resting-state fMRI data were pre-processed using the in-house Brainnetome fMRI Toolkit (http://www.brainnetome.org/brainnetometool) based on Statistical Parametric Mapping (SPM8, http://www.fil.ion.ucl.ac.uk/spm). Pre-processing steps included (1) slice-timing correction; (2) realignment to the first volume for head motion correction; (3) spatial normalization to a standard EPI template with re-slicing to 2 mm cubic voxels; (4) regression of nuisance parameters including linear drift, six motion parameters, and the mean time series of all voxels within the white matter and cerebrospinal fluid; (5) temporal filtering (0.01–0.08 Hz) to reduce high frequency and low frequency noise; (6) spatial smoothing with a Gaussian kernel (full-width-at-half-maximum [FWHM] 6 mm) [40–43].

The difference in gray matter volume between patients and normal controls may impact on functional connectivity [44, 45]. In order to control for this confounding variable, we performed voxel-based morphometry (VBM) analysis using the VBM8 toolbox (http://dbm.neuro.uni-jena.de/vbm/). The structural images were preprocessed through standard steps [46]. First, the subjects' T1-weighted images were aligned with the ICBM template and were tissue-segmented according to the tissue probability map provided in VBM8. Second, the segmented GM was modulated by the non-linear normalization parameters to correct for individual brain size. Finally, the modulated and warped GM was smoothed by convolving with an isotropic Gaussian kernel (8 mm FWHM). The resulting gray matter volume was used as a covariate in the statistical analysis.

Regions of interest

In the present study, 36 voxels' MNI coordinates taken from the study by Brier and colleagues [38] were used to generate regions of interest (ROIs) (for details see Supplementary Table 1). These ROIs were derived by maximizing the topographic concordance between results obtained by ROI connectivity

mapping and by spatial independent component analysis [38]. Then, 36 6-mm-radius spherical ROIs centered on these coordinates were produced (Supplementary Figure 1). We extracted the mean time series within each ROI from the smoothed normalized fMRI time series for each subject. These ROIs represent seven brain networks corresponding to primary auditory, primary visual, somatomotor, DMN, DAN, SAL, and CON. Primary auditory, primary visual, and somatomotor areas were further integrated into a single sensory-motor network (SMN) for consistency with previous studies [38, 47], yielding five RSNs for subsequent analysis: DMN, DAN, SAL, CON, and SMN.

Estimation of regional functional connectivity

The Pearson's correlation coefficients between mean time series of each pair of ROIs were computed for each subject. The correlation coefficients were converted to η values using an exponential function related to the connectivity "distance" between the two connected ROIs [48]. This step insured that all of the correlations were positive, which was necessary for the analysis of the changes between baseline and follow-up. Specifically, the conversion was $\eta_{ij} = e^{-\xi d_{ij}}$, where $\xi = 2$ is a positive constant [49], $d_{ij} = \left(1 - r_{ij}\right) / \left(1 + r_{ij}\right)$ is a hyperbolic correlation measure [50] denoting the distance between two nodes, and r_{ij} is the Pearson's correlation coefficient. Using these measures, we proceeded at three levels of analysis:

i) 'nodal integration': The total connectivity degree, Γ, of node i was calculated using $\Gamma_i = \sum_{j=1}^{n} \eta_{ij}$ [49] as the measurement of nodal integration, i.e., each node's connectivity with the rest of the brain. This measure is equivalent to the weighted degree of the node in graph theory.
ii) 'RSN profile': Intra- and inter- network analyses were performed as previously described [38]. The intra-network composite score, c, was defined by averaging the transformed correlation coefficients of all ROI pairs in a particular RSN as $c^N = \langle \eta_{ij} \rangle$, where i and j refer to ROIs in a particular network N and<>denotes the mean across ROI pairs. The inter-network composite score, c, was calculated by averaging the transformed correlation coefficients of all ROI pairs belonging to different RSNs as $c^{X,Y} = \langle \eta_{ij} \rangle$, where X and Y denote separate networks, i refers to an ROI in X, and j refers to an ROI in Y [38].
iii) 'large-scale connectivity': Treating correlated brain regions as networks achieves data reduction and reduces the effect of sampling error across pairs of nodes, but this step may also obscure focal phenomena [38]. To address this concern, we further investigated the functional connectivity between all the possible pairs of ROIs. In other words, for the selected 36 ROIs, we evaluated the disrupted connectivity profile for each of the 630 ROI pairs among the three participant groups [43].

Statistical analysis

For each level of analysis, one-way analysis of variance (ANOVA) was performed for a group-wise comparison between the NC, EMCI, and LMCI groups after regressing out age, gender, APOE genotype and interactions between them as well as gray matter volume effects, both at the baseline visit and the follow up and longitudinal changes between them. A permutation test was used to control for Type I error. Specifically, for each connectivity measure, the test statistic was computed first for the actual experimental groups. Then, 10,000 permutations of group membership were performed, and the statistics were recalculated for the permuted groups to yield an empirical distribution of the test statistic. The permutation p value was determined by computing the proportion of the 10,000 permutations for which the permuted test statistic was greater than the original test statistic. *Post hoc* Student's t-test were also performed.

To determine whether connectivity measures were correlated with cognitive ability, Pearson's correlation coefficients were calculated between cognitive scores and the connectivity measures in MCI patients. Bootstrapping methods were applied to obtain the 95% confidence interval (CI) of the correlation coefficients. Briefly, the MCI population was resampled with replacement 10,000 times and correlation coefficients were calculated for each resample to generate the 95% CI. If the CI does not contain zero, this is an indication that the observed correlation is statistically significant.

RESULTS

Cognitive and neuropsychological tests

According to the inclusion and exclusion criteria, 68 subjects were included in the study.

There were no significant differences in gender ($\chi^2_2 = 3.48$, p = 0.139) or age ($p = 0.400$ for the first visit and 0.392 for the second) among the NC, EMCI, and LMCI groups. The averaged MMSE score was 29.2 ± 1.0 for NC group, 28.3 ± 1.2 for EMCI group and 27.6 ± 1.2 for LMCI at the baseline visit (ANOVA, $p = 0.002$). Compared to normal controls, MCI patients exhibited deficits in modified ADAS-Cog both at baseline ($p < 0.001$) and follow-up ($p < 0.001$) (mean ADAS-Cog 7.7 ± 4.3 for NC, 11.6 ± 6.1 for EMCI, and 17.4 ± 6.5 for LMCI at baseline; Table 1).

It has been reported that small amounts of head-motion during data scanning can have a substantial impact on estimations of functional connectivity and functional networks in the resting brain [51–54]. Therefore, we excluded subjects with translations or rotation larger than the size of one voxel in each scan. We also evaluated group differences in head motion among the three groups according to the criteria of Van Dijk and colleagues [53]. The results showed that the three groups had no significant differences in head motion (Table 1).

Nodal integration

For each ROI, we tested for group differences in nodal functional connectivity strength at each of the two time visits as well as for longitudinal changes between visits. Two regions of DAN (laIPS and raIPS) and three regions of SMN (rMC, SMA and lA1) showed significantly lower nodal strength in MCI comparing to NC in the original visit (Supplementary Figures 2A–E). Widely distributed regions (PCC, riTmp, laIPS, dmPFC, rACC, SMA, rV1, and lA1) showed significant correlations with ADAS-Cog (Supplementary Figures 2F-M and Supplementary Table 2). Nodal strength of two regions (riTmp and rPut) were affected in MCI patients at the follow-up visit (Supplementary Figures 3A, B). Additionally, three regions (lLP, lV1, and rV1) showed significant correlations between nodal strength and ADAS-Cog

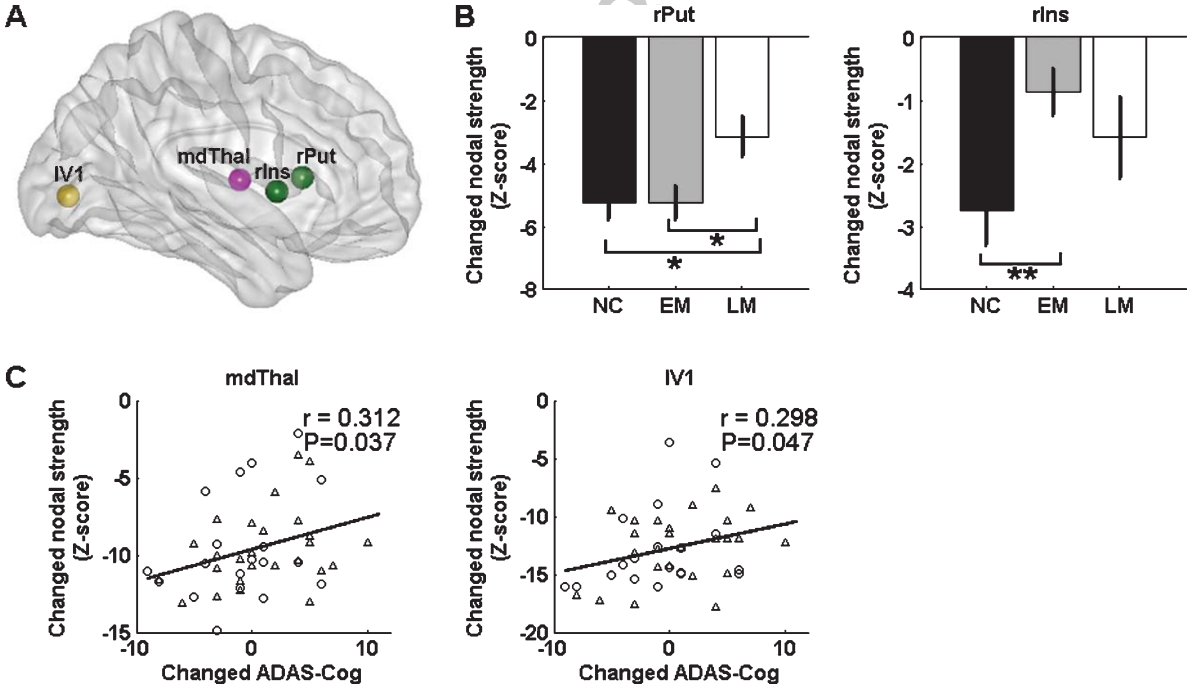

Fig. 2. Disease-related alterations in nodal degree. A) Individual regions of interest are displayed on the brain surface. Dark green spheres represent the ROIs (rPut and rIns) in SAL which were statistically significant in one-way ANOVA. The pink sphere represents the ROI (mdThal) in DMN whose nodal degree was significantly correlated with changes in ADAS-Cog scores. The golden sphere represents the ROI (lV1) in SMN whose nodal degree was significantly correlated with changes in ADAS-Cog scores. B) rPut and rIns showed significant group differences. *Post hoc* comparisons between each pair of two groups were performed using Student's *t*-test, with significant differences indicated as $^{*}p < 0.05$ and $^{**}p < 0.01$. NC, normal control; EM, early MCI; LM, late MCI. (C) Scatterplots showing the two regions in terms of statistical significance for the correlation between changes in nodal strength and changes in ADAS-Cog scores. Triangles represent EMCI, and circles represent LMCI. Abbreviations can be found in Supplementary Table 1.

Table 2
Correlations between changes in connectivity strength and changes in ADAS-Cog score

		CI lower	CI upper	Observed R	Observed P
Nodal	mdThal	0.073	0.522	0.312	0.037
	lV1	0.027	0.534	0.298	0.047
RSN	DMN	0.066	0.560	0.331	0.026

CI, confidence interval; mdThal, medial thalamus; lV1, left primary visual; RSN, resting-state network; DMN, default mode network.

scores at the follow-up visit (Supplementary Figures 3C–E and Supplementary Table 2). The changes in nodal strength between visits showed significant group differences in two regions of the SAL network, rPut (permutation test, $p = 0.022$) and rIns (permutation test, $p = 0.030$) (Figs. 2A, B). *Post hoc* analysis further showed that the main effect of group was between NC and LMCI and between EMCI and LMCI in rPut, while the main effect was between NC and EMCI in rIns. Furthermore, the changes in nodal strength in mdThal ($r = 0.312$, 95% CI: 0.073, 0.312) and lV1 ($r = 0.298$, 95% CI: 0.027, 0.534) were strongly positively related to the changes in ADAS-Cog score (Figs. 2A, C; Table 2).

RSN profile: Intra-network connectivity

One-way ANOVA was performed on each individual RSN for each of the two time visits as well for the longitudinal change between visits. SMN, showed statistically significant group differences at the baseline visit (permutation test $p = 0.023$, Supplementary Figure 4A). There was a trend towards group differences in DAN ($p = 0.052$) between the three groups. The lower composite z-scores of SMN ($r = –0.389$, 95% CI: –0.612, –0.145) and CON ($r = –0.308$ 95% CI: –0.499, –0.137) were associated with greater ADAS-Cog scores (Supplementary Figures 4B, C; Supplementary Table 3). No RSN in the follow-up was found abnormal either one-way ANOVA or correlation with ADAS-Cog at statistical level of 0.05. However, change in composite score of the DMN ($r = 0.331$, 95% CI: 0.066, 0.56) was related to change in ADAS-Cog from follow-up to baseline (Fig. 3A).

RSN profile: Inter-network connectivity

On the original visit, we found that the connectivity strength between the DAN and SMN showed significant group differences, with a difference between NC and LMCI driving the overall effect (Supplementary Figures 4D, E). In addition, the inter-network correlations of DMN-SAL, DMN-SMN, and DAN-SMN were significantly correlated with ADAS-Cog scores (Supplementary Figures 4D, F, H; Supplementary Table 3). There were no significant abnormalities in inter-network correlation at the follow-up visit. To quantify the longitudinal effects, we evaluated differences in longitudinal alterations across RSNs between the three groups. The change in correlation strength of the DMN-SAL pair (permutation test, $p = 0.041$) was identified to be affected with the main effect between the NC and LMCI groups (Figs. 3B, C).

Large-scale connectivity

At the baseline visit, abnormal functional connectivities were distributed widely between brain

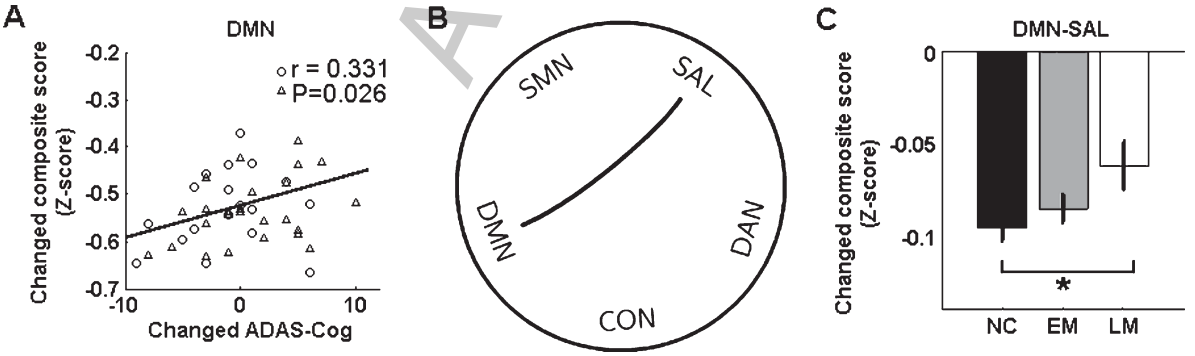

Fig. 3. Impairment of the intra- and inter-network RSN profile. A) The DMN shows significant correlation between intra-network connectivity and changes in ADAS-Cog score. B) Circles contain the RSN name; abbreviations denote five RSNs; lines indicate that the inter-network functional connectivity was significantly different between the three groups. C) The change in correlation strength between DMN and SAL showed significant group differences ($p = 0.007$). *Post hoc* comparisons between each pair of two groups were performed using Student's *t*-test, with significant differences indicated as $^*p < 0.05$.

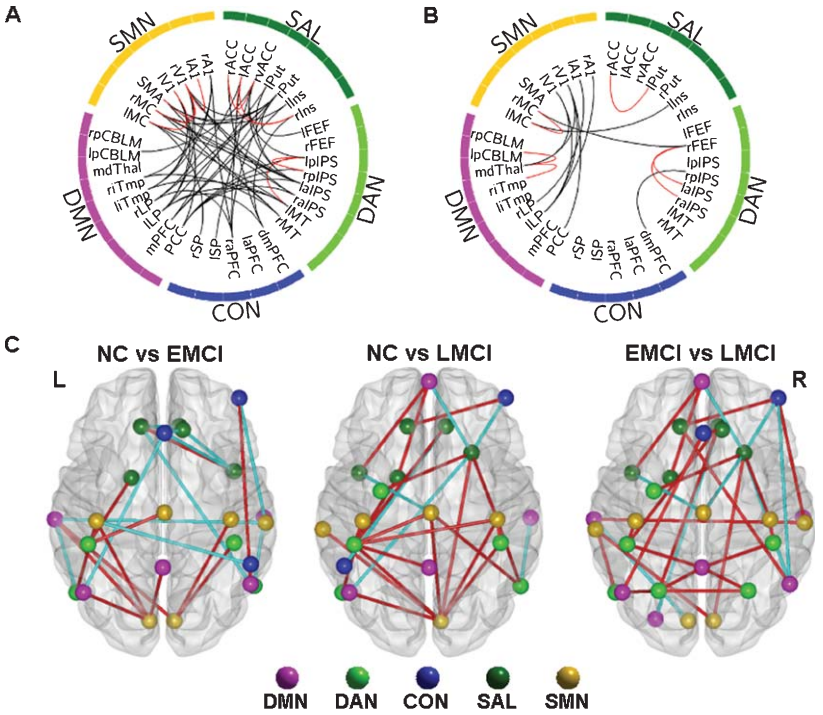

Fig. 4. Abnormal longitudinal alterations in functional connectivity for all ROI pairs (large-scale connectivity level). In the upper row, the circle is comprised of five arcs that represent five RSNs, and each arc is comprised of the ROIs that are part of that RSN. Lines denote abnormal connectivity between connected ROIs: Red lines indicate that the ROIs are part of the same RSN, while black lines denote that the ROIs are part of different RSNs. A) Changes in connectivity were significantly different between the three groups (permutation test $p < 0.05$). B) Changes in connectivity were correlated with changes in ADAS-Cog scores in subjects with MCI (95% CI did not include zero). C) *Post hoc* analysis demonstrated altered connectivity between each pair of two groups, displayed on the brain surface. Colored nodes represent ROIs in different RSNs. Red lines indicate that changes in connectivity strength in the first group are greater than the second group (e.g., NC > EMCI in the left-most figure), while cyan lines indicate that changes in connectivity strength in the first group are less than the second group (e.g., NC < EMCI in the left-most figure). Abbreviations can be found in Supplementary Table 1.

regions. The disrupted intra-network ROI connectivities were mainly concentrated in DAN and SMN, and the disrupted inter-network ROI connectivities mainly involved the DAN-SMN pair (Supplementary Figure 5A, Supplementary Table 4). *Post hoc* analysis revealed that the main effects were between NC and LMCI, and between EMCI and LMCI (Supplementary Figure 5C). Moreover, connectivity strength was associated with severity of cognitive impairment in MCI. The correlation between connectivity strength and ADAS-Cog score mostly involved PCC, riTmp, dmPFC, and SMA (Supplementary Figure 5B and Supplementary Table 4).

At the follow-up visit, the large-scale connectivity results showed disrupted connectivity distributed throughout the brain but most particularly involving riTmp and rPut (Supplementary Figure 6A and Supplementary Table 5). The group differences were mainly between NC and LMCI, and between EMCI and LMCI (Supplementary Figure 6C). Connectivity correlations with ADAS-Cog principally involved lLP, lV1, and rV1 (Supplementary Figure 6B and Supplementary Table 5).

In order to investigate the disrupted functional connectivity in MCI patients, we evaluated the longitudinal alterations of functional connectivity in MCI compared to NC. Our results showed abnormalities in intra-network ROI connectivity (mainly involving SAL and SMN) and abnormalities in inter-network ROI connectivity (mainly involving the DMN-SAL and DAN-SMN pairs) (Fig. 4A and Supplementary Table 6). The longitudinal alterations of functional connectivity in EMCI were greater than those observed in LMCI (Fig. 4C). Few ROI pairs showed correlations between changes in connectivity strength and changes in ADAS-Cog score (Fig. 4B and Supplementary Table 6).

DISCUSSION

The main innovation of the present study is the analysis of intra- and inter-network connectivity patterns at three parallel levels of analysis, from nodal to large-scale connectivity, in a large, clinically graded, longitudinal sample including early and late MCI. This study is also novel in elucidating that longitudinal change in intra- and inter-network connectivity is associated with change in symptomatic impairment measured in the MCI group. These alterations in intra- and inter-network brain organization complement the aberrant brain network architecture observed in subjects at high risk for AD.

Disrupted intra-network connectivity within individual RSNs

The human brain at rest is organized as a complex system with different functional modules termed RSNs—such as DMN, DAN, CON, SAL, and SMN—which are both specialized for processing distinct forms of information and integrated to fulfill the functions of daily life. These vital networks have been hypothesized to be vulnerable to diseases such as MCI/AD [17, 38, 55]. The present study supports this hypothesis by showing alterations within the DMN in a longitudinal analysis of MCI patients. The change in connectivity strength within the DMN was correlated with the change in cognitive ability measured by ADAS-Cog (Fig. 3A). The connectivity strengths of PCC and of riTmp, a core hub region of DMN [56], demonstrated significant associations with cognitive ability (Supplementary Figure 2F, G). Another important region in the DMN, mdThal, showed significant correlations between changes in nodal degree and changes ADAS-Cog score (Fig. 2C). The DMN is associated with self-referential, episodic memory [23, 57, 58], possibly representing the core network targeted in MCI/AD subjects [17, 21, 43, 59, 60]. Our findings reveal that the regional interactions within the DMN become disrupted in early cognitive impairment, confirming the important status of this network for understanding the pathophysiological process of AD.

With disease progression, other representative RSNs become compromised, notably SAL. Our results demonstrate that the rIns and rPut, important regions of the salience network, show significant group differences in nodal strength (Fig. 2B). SAL is involved in the important function of detecting and adapting to salient external stimuli and internal events [61, 62]. Specifically, the insula, an integral hub region in SAL, detects stimulus signals and initiates control signals to coordinate brain activity [36, 37, 63]. Our findings are supported by recent studies of the insula, which revealed regional atrophy and accumulation of Aβ in MCI [64], as well as gray matter loss and functional connectivity reduction in AD [65]. The impaired functional connectivity of this region may result in impaired functional connectivity throughout SAL and other brain networks.

Dysfunctions in sensory or motor networks are often taken as normal signs of aging, when in fact this dysfunction may represent an early sign of AD. AD patients suffer from sensory, cognitive, and motor impairments. A recent study revealed impaired connectivity between the thalamus and the rest of the visual system in EMCI and LMCI, suggesting reduced functional integrity of the visual system [66]. A recent review also emphasized the importance of sensory and motor regions to AD pathology [32]. In the present study, intriguingly, we observe significant group differences in connectivity strength of SMN at all three levels of analysis (Supplementary Figures 2, 4, and 5). Moreover, differences in SMN (including important regions such as SMA, rV1 and lA1) were associated with alterations in ADAS-Cog score both at baseline (Supplementary Figures 2 and 4) and longitudinally between visits (Fig. 2C). These findings are supported by previous evidence that neurofibrillary tangles and Aβ plaques in AD may result in dysfunction of visual cortex [67, 68]. Moreover, SMN participates with supramarginal gyrus in modulating action recognition and episodic memory [69, 70], impairment of which is one of the key features of AD [71, 72]. Taken together, these results suggest that SMN abnormalities may facilitate the early diagnosis of AD.

Disrupted inter-network connectivity between RSNs

The human brain is a complex hierarchical system that coordinates a variety of specific functions, depending on a balance between local processing and global integration of information. Efficient behavior involves the coordinated activity of brain networks, and this coordination is the biological cornerstone for daily human cognition [33]. This coordination may represent the dynamic interaction of networks as reflected by the connectivity between RSNs [18, 73]. It has been proposed that abnormal cognition results

from a disruption in the balance between different brain systems in AD/MCI [74, 75].

Previous cross-sectional studies have demonstrated inter-network disconnections between SAL, CON, and DMN associated with cognitive decline from normal aging to MCI and eventually to AD [65, 76]. In the present study, there was evidence of longitudinal change in DMN-SAL connectivity strength in MCI (Figs. 3, 4). Moreover, inter-network correlation strength (DAN-SMN, DMN-SAL and DMN-SMN pairs) was progressively reduced with disease progression (Supplementary Figures 4 and 5). These findings are supported by previous studies which have provided convergent evidence that not only functional connectivity within RSNs but also between RSNs was impaired in patients with MCI/AD [17, 38, 77, 78]. Notably, two of these three RSN pairs involved the DMN. As discussed above, DMN consists of a set of core hub region that play a key role in modulating daily cognition [59]. It has been proposed that the dysfunction of one network may initiate disordered outputs to other networks, which are initially unaffected by the disease [38, 79]. This is in line with a recent study which supports the hypothesis of the transneuronal spread model that some toxic agents travel between networks [80]. Convergence evidence has revealed that the salience network can causally influence activity of the DMN [81, 82] and mediate engagement and disengagement of corresponding brain regions in response to stimuli [36], a process which is thought to be crucial for cognitive control and daily cognition [35, 83, 84]. Therefore, we speculate that the SAL and SMN are necessary for the efficient regulation of activity in the DMN. A disturbance of this regulation may lead to inefficient cognitive control in MCI. Collectively, our results support the hypothesis that disruption between RSNs begins in networks that are affected early in the disease (i.e., DMN) and subsequently spreads to other networks. This hypothesis needs to be tested in future longitudinal studies.

Disruption and compensatory mechanism coexist in patients with MCI

Accumulating functional imaging evidence suggests that increased recruitment of brain regions may be a compensatory response in patients with cognitive impairment [85–87]. In the present study, we observed significant correlations between changes in connectivity strength within DMN and changes in ADAS-Cog scores in patients with MCI (Fig. 3A), which indicates that reduction of functional connectivity was correlated with cognitive impairment in MCI and AD [43]. This disrupted functional connectivity is a potential biomarker of cognitive impairment in MCI [17]. Additionally, the change in connectivity strength from follow-up to baseline was greater in EMCI patients than in LMCI patients, possibly because of a recruitment of other brain regions to compensate for functional deficits in LMCI. These conclusions are supported by previous cross-sectional studies in which compensatory increases in brain connectivity were identified in AD/MCI subjects [87–89]. Patterns of disruption and compensation may co-exist during the prodromal stage of AD. Taken together, these results strengthen the conclusion that interventions that either prevent disruptions or strengthen compensatory responses could delay conversion to AD.

Methodological considerations

One methodological consideration in our analysis was that the Pearson's correlation coefficient was converted to the correlation index using an exponential transformation [49]. The advantage of this method is that negative correlations were transformed to positive values, to avoid the offsetting of positive and negative correlations when investigating mean effects. However, negative correlations exist intrinsically between different networks [90], and the amplitude of negative correlations in different networks varies as a function of frequency [91], indicating an elusive biological role for negatively-correlated brain activity in need of further investigation.

Our study addressed potential confounds of genotype and brain atrophy on the functional connectivity analysis. We elected to use of APOE genotype as an inclusion criterion. The APOE $\varepsilon 4$ allele is associated with increased risk for AD and has potential effects on both brain activity [20] and functional connectivity [39]. Therefore, it was important to correct for the effect of genotype on functional connectivity. As for brain atrophy, although we corrected for total brain volume, localized atrophy in early AD could still confound results. If a volume of interest contained fewer gray matter voxels, then the fMRI signal would be predicted to be noisier. Therefore, in a reanalysis we corrected for the gray matter of individual volumes of interest (Supplementary Figure 7), showing convergent results with the original analysis.

Several other methodological limitations existed in the present study. 1) Only 140 fMRI volumes were used for each subject, which is a relatively short scan length and may result in relatively low signal-to-noise (SNR) in the fMRI analysis. To address this issue, we conducted a supplementary analysis demonstrating that the temporal signal-to-noise (tSNR) [92] in the selected regions is acceptable (Supplementary Figure 8). 2) The correlation analysis between functional connectivity and clinical variables (ADAS-Cog) may be susceptible to Type I error. Our use of an uncorrected p-value threshold of 0.05 combined with a permutation test (in the ANOVA analysis) and a bootstrap procedure (in the correlation analysis) was designed to limit Type I error, and we note that many results far exceeded this nominal threshold. 3) The EMCI patients and the LMCI patients were combined into one group to investigate the relationship between cognitive performance and functional connectivity, so between group differences could be contributing to the relationships that we report. Sub-group analysis revealed trend-level but not statistically significant correlations within each group separately, possibly due to the relatively small sample sizes and the limited ability of ADAS-Cog to detect subtle cognitive changes. 4) We included only two scans for each subject and limited the analysis to patients who did not change diagnostic groups between baseline and follow up visits. Future analyses could expand this area of analysis, for example, by looking explicitly at intra- and inter-network connectivity in subjects who progressed to AD at follow up. 5) Finally, the present study was an ROI-based analysis. Because the regions of interest were defined a priori, group differences may well exist in other parts of the brain. Further investigations using finer brain parcellations should be conducted in the future.

ACKNOWLEDGMENTS

This work was partially supported by the Natural Science Foundation of China (Nos. 81571062, 81270020, 81471120, 81371544, 61305143); the Natural Science Foundation of Beijing (No. 7152096); the Youth Innovation Promotion Association CAS (No. 2014119); the Beijing Nova Program (No. Z151100003150112); and the Open Project Program of the National Laboratory of Pattern Recognition (No. 201407344).

Data collection and sharing for this project was funded by the Alzheimer's Disease Neuroimaging Initiative (ADNI) (National Institutes of Health Grant U01 AG024904) and DOD ADNI (Department of Defense award number W81XWH-12-2-0012). ADNI is funded by the National Institute on Aging, the National Institute of Biomedical Imaging and Bioengineering, and through generous contributions from the following: AbbVie, Alzheimer's Association; Alzheimer's Drug Discovery Foundation; Araclon Biotech; BioClinica, Inc.; Biogen; Bristol-Myers Squibb Company; CereSpir, Inc.; Eisai Inc.; Elan Pharmaceuticals, Inc.; Eli Lilly and Company; EuroImmun; F. Hoffmann-La Roche Ltd and its affiliated company Genentech, Inc.; Fujirebio; GE Healthcare; IXICO Ltd.; Janssen Alzheimer Immunotherapy Research & Development, LLC.; Johnson & Johnson Pharmaceutical Research & Development LLC.; Lumosity; Lundbeck; Merck & Co., Inc.; Meso Scale Diagnostics, LLC.; NeuroRx Research; Neurotrack Technologies; Novartis Pharmaceuticals Corporation; Pfizer Inc.; Piramal Imaging; Servier; Takeda Pharmaceutical Company; and Transition Therapeutics. The Canadian Institutes of Health Research is providing funds to support ADNI clinical sites in Canada. Private sector contributions are facilitated by the Foundation for the National Institutes of Health (http://www.fnih.org). The grantee organization is the Northern California Institute for Research and Education, and the study is coordinated by the Alzheimer's Disease Cooperative Study at the University of California, San Diego. ADNI data are disseminated by the Laboratory for Neuro Imaging at the University of Southern California.

Authors' disclosures available online (http://www.j-alz.com/manuscript-disclosures/16-0008).

SUPPLEMENTARY MATERIAL

The supplementary material is available in the electronic version of this article: http://dx.doi.org/10.3233/JAD-160008.

REFERENCES

[1] Sperling RA, Aisen PS, Beckett LA, Bennett DA, Craft S, Fagan AM, Iwatsubo T, Jack CR Jr, Kaye J, Montine TJ, Park DC, Reiman EM, Rowe CC, Siemers E, Stern Y, Yaffe K, Carrillo MC, Thies B, Morrison-Bogorad M, Wagster MV, Phelps CH (2011) Toward defining the preclinical stages of Alzheimer's disease: Recommendations from the National Institute on Aging-Alzheimer's Association workgroups on diagnostic guidelines for Alzheimer's disease. *Alzheimers Dement* **7**, 280-292.

[2] Jack CR Jr, Knopman DS, Jagust WJ, Petersen RC, Weiner MW, Aisen PS, Shaw LM, Vemuri P, Wiste HJ, Weigand SD, Lesnick TG, Pankratz VS, Donohue MC, Trojanowski JQ (2013) Tracking pathophysiological processes in Alzheimer's disease: An updated hypothetical model of dynamic biomarkers. *Lancet Neurol* **12**, 207-216.

[3] Jack CR Jr, Albert MS, Knopman DS, McKhann GM, Sperling RA, Carrillo MC, Thies B, Phelps CH (2011) Introduction to the recommendations from the National Institute on Aging-Alzheimer's Association workgroups on diagnostic guidelines for Alzheimer's disease. *Alzheimers Dement* **7**, 257-262.

[4] Petersen RC (2011) Clinical practice. Mild cognitive impairment. *N Engl J Med* 2227-2234.

[5] Petersen RC, Smith GE, Waring SC, Ivnik RJ, Tangalos EG, Kokmen E (1999) Mild cognitive impairment: Clinical characterization and outcome. *Arch Neurol* **56**, 303-308.

[6] Fischer P, Jungwirth S, Zehetmayer S, Weissgram S, Hoenigschnabl S, Gelpi E, Krampla W, Tragl KH (2007) Conversion from subtypes of mild cognitive impairment to Alzheimer dementia. *Neurology* **68**, 288-291.

[7] Gauthier S1, Reisberg B, Zaudig M, Petersen RC, Ritchie K, Broich K, Belleville S, Brodaty H, Bennett D, Chertkow H, Cummings JL, de Leon M, Feldman H, Ganguli M, Hampel H, Scheltens P, Tierney MC, Whitehouse P, Winblad B, International Psychogeriatric Association Expert Conference on mild cognitive impairment (2006) Mild cognitive impairment. *Lancet* **367**, 1262-1270.

[8] Maioli F, Coveri M, Pagni P, Chiandetti C, Marchetti C, Ciarrocchi R, Ruggero C, Nativio V, Onesti A, D'Anastasio C, Pedone V (2007) Conversion of mild cognitive impairment to dementia in elderly subjects: A preliminary study in a memory and cognitive disorder unit. *Arch Gerontol Geriatr* **44**(Suppl 1), 233-241.

[9] Petersen RC (2009) Early diagnosis of Alzheimer's disease: Is MCI too late? *Curr Alzheimer Res* **6**, 324-330.

[10] Aisen PS, Petersen RC, Donohue MC, Gamst A, Raman R, Thomas RG, Walter S, Trojanowski JQ, Shaw LM, Beckett LA, Jack CR Jr, Jagust W, Toga AW, Saykin AJ, Morris JC, Green RC, Weiner MW, Alzheimer's Disease Neuroimaging, Initiative (2010) Clinical Core of the Alzheimer's Disease Neuroimaging Initiative: Progress and plans. *Alzheimers Dement* **6**, 239-246.

[11] Weiner MW, Aisen PS, Jack CR Jr, Jagust WJ, Trojanowski JQ, Shaw L, Saykin AJ, Morris JC, Cairns N, Beckett LA, Toga A, Green R, Walter S, Soares H, Snyder P, Siemers E, Potter W, Cole PE, Schmidt M, Alzheimer's Disease Neuroimaging Initiative (2010) The Alzheimer's disease neuroimaging initiative: Progress report and future plans. *Alzheimers Dement* **6**, 202-211 e207.

[12] Biswal B, Yetkin FZ, Haughton VM, Hyde JS (1995) Functional connectivity in the motor cortex of resting human brain using echo-planar MRI. *Magn Reson Med* **34**, 537-541.

[13] Smith SM, Fox PT, Miller KL, Glahn DC, Fox PM, Mackay CE, Filippini N, Watkins KE, Toro R, Laird AR, Beckmann CF (2009) Correspondence of the brain's functional architecture during activation and rest. *Proc Natl Acad Sci U S A* **106**, 13040-13045.

[14] Fox MD, Raichle ME (2007) Spontaneous fluctuations in brain activity observed with functional magnetic resonance imaging. *Nat Rev Neurosci* **8**, 700-711.

[15] Damoiseaux JS, Rombouts SA, Barkhof F, Scheltens P, Stam CJ, Smith SM, Beckmann CF (2006) Consistent resting-state networks across healthy subjects. *Proc Natl Acad Sci U S A* **103**, 13848-13853.

[16] Liao W, Mantini D, Zhang Z, Pan Z, Ding J, Gong Q, Yang Y, Chen H (2010) Evaluating the effective connectivity of resting state networks using conditional Granger causality. *Biol Cybern* **102**, 57-69.

[17] Sorg C, Riedl V, Muhlau M, Calhoun VD, Eichele T, Laer L, Drzezga A, Forstl H, Kurz A, Zimmer C, Wohlschlager AM (2007) Selective changes of resting-state networks in individuals at risk for Alzheimer's disease. *Proc Natl Acad Sci U S A* **104**, 18760-18765.

[18] Yeo BT, Krienen FM, Sepulcre J, Sabuncu MR, Lashkari D, Hollinshead M, Roffman JL, Smoller JW, Zollei L, Polimeni JR, Fischl B, Liu H, Buckner RL (2011) The organization of the human cerebral cortex estimated by intrinsic functional connectivity. *J Neurophysiol* **106**, 1125-1165.

[19] Mantini D, Perrucci MG, Del Gratta C, Romani GL, Corbetta M (2007) Electrophysiological signatures of resting state networks in the human brain. *Proc Natl Acad Sci U S A* **104**, 13170-13175.

[20] Filippini N, MacIntosh BJ, Hough MG, Goodwin GM, Frisoni GB, Smith SM, Matthews PM, Beckmann CF, Mackay CE (2009) Distinct patterns of brain activity in young carriers of the APOE-epsilon4 allele. *Proc Natl Acad Sci U S A* **106**, 7209-7214.

[21] Greicius MD, Srivastava G, Reiss AL, Menon V (2004) Default-mode network activity distinguishes Alzheimer's disease from healthy aging: Evidence from functional MRI. *Proc Natl Acad Sci U S A* **101**, 4637-4642.

[22] Wang P, Zhou B, Yao H, Zhan Y, Zhang Z, Cui Y, Xu K, Ma J, Wang L, An N, Zhang X, Liu Y, Jiang T (2015) Aberrant intra- and inter-network connectivity architectures in Alzheimer's disease and mild cognitive impairment. *Sci Rep* **5**, 14824.

[23] Buckner RL, Snyder AZ, Shannon BJ, LaRossa G, Sachs R, Fotenos AF, Sheline YI, Klunk WE, Mathis CA, Morris JC, Mintun MA (2005) Molecular, structural, and functional characterization of Alzheimer's disease: Evidence for a relationship between default activity, amyloid, and memory. *J Neurosci* **25**, 7709-7717.

[24] Wang L, Zang Y, He Y, Liang M, Zhang X, Tian L, Wu T, Jiang T, Li K (2006) Changes in hippocampal connectivity in the early stages of Alzheimer's disease: Evidence from resting state fMRI. *Neuroimage* **31**, 496-504.

[25] Liu J, Zhang X, Yu C, Duan Y, Zhuo J, Cui Y, Liu B, Li K, Jiang T, Liu Y (2015) Impaired parahippocampus connectivity in mild cognitive impairment and Alzheimer's disease. *J Alzheimers Dis* **49**, 1051-1064.

[26] Bell-McGinty S, Lopez OL, Meltzer CC, Scanlon JM, Whyte EM, Dekosky ST, Becker JT (2005) Differential cortical atrophy in subgroups of mild cognitive impairment. *Arch Neurol* **62**, 1393-1397.

[27] Jin M, Pelak VS, Cordes D (2012) Aberrant default mode network in subjects with amnestic mild cognitive impairment using resting-state functional MRI. *Magn Reson Imaging* **30**, 48-61.

[28] Bai F, Watson DR, Shi Y, Wang Y, Yue C, YuhuanTeng, Wu D, Yuan Y, Zhang Z (2011) Specifically progressive deficits of brain functional marker in amnestic type mild cognitive impairment. *PLoS One* **6**, e24271.

[29] Damoiseaux JS, Prater KE, Miller BL, Greicius MD (2012) Functional connectivity tracks clinical deterioration in Alzheimer's disease. *Neurobiol Aging* **33**, 828 e819-830.

[30] Corbetta M, Shulman GL (2002) Control of goal-directed and stimulus-driven attention in the brain. *Nat Rev Neurosci* **3**, 201-215.

[31] Zhang Z, Zheng H, Liang K, Wang H, Kong S, Hu J, Wu F, Sun G (2015) Functional degeneration in dorsal and ventral attention systems in amnestic mild cognitive impairment and Alzheimer's disease: An fMRI study. *Neurosci Lett* **585**, 160-165.

[32] Albers MW, Gilmore GC, Kaye J, Murphy C, Wingfield A, Bennett DA, Boxer AL, Buchman AS, Cruickshanks KJ, Devanand DP, Duffy CJ, Gall CM, Gates GA, Granholm AC, Hensch T, Holtzer R, Hyman BT, Lin FR, McKee AC, Morris JC, Petersen RC, Silbert LC, Struble RG, Trojanowski JQ, Verghese J, Wilson DA, Xu S, Zhang LI (2015) At the interface of sensory and motor dysfunctions and Alzheimer's disease. *Alzheimers Dement* **11**, 70-98.

[33] Bullmore E, Sporns O (2012) The economy of brain network organization. *Nat Rev Neurosci* **13**, 336-349.

[34] Bullmore E, Sporns O (2009) Complex brain networks: Graph theoretical analysis of structural and functional systems. *Nat Rev Neurosci* **10**, 186-198.

[35] Menon V (2011) Large-scale brain networks and psychopathology: A unifying triple network model. *Trends Cogn Sci* **15**, 483-506.

[36] Menon V, Uddin LQ (2010) Saliency, switching, attention and control: A network model of insula function. *Brain Struct Funct* **214**, 655-667.

[37] Uddin LQ (2015) Salience processing and insular cortical function and dysfunction. *Nat Rev Neurosci* **16**, 55-61.

[38] Brier MR, Thomas JB, Snyder AZ, Benzinger TL, Zhang D, Raichle ME, Holtzman DM, Morris JC, Ances BM (2012) Loss of intranetwork and internetwork resting state functional connections with Alzheimer's disease progression. *J Neurosci* **32**, 8890-8899.

[39] Wang X, Wang J, He Y, Li H, Yuan H, Evans A, Yu X, He Y, Wang H (2015) Apolipoprotein E epsilon4 modulates cognitive profiles, hippocampal volume, and resting-state functional connectivity in Alzheimer's disease. *J Alzheimers Dis* **45**, 781-795.

[40] Zhang Z, Liu Y, Jiang T, Zhou B, An N, Dai H, Wang P, Niu Y, Wang L, Zhang X (2012) Altered spontaneous activity in Alzheimer's disease and mild cognitive impairment revealed by Regional Homogeneity. *Neuroimage* **59**, 1429-1440.

[41] Yao H, Liu Y, Zhou B, Zhang Z, An N, Wang P, Wang L, Zhang X, Jiang T (2013) Decreased functional connectivity of the amygdala in Alzheimer's disease revealed by resting-state fMRI. *Eur J Radiol* **82**, 1531-1538.

[42] Zhou B, Liu Y, Zhang Z, An N, Yao H, Wang P, Wang L, Zhang X, Jiang T (2013) Impaired functional connectivity of the thalamus in Alzheimer's disease and mild cognitive impairment: A resting-state FMRI study. *Curr Alzheimer Res* **10**, 754-766.

[43] Liu Y, Yu C, Zhang X, Liu J, Duan Y, Alexander-Bloch AF, Liu B, Jiang T, Bullmore E (2014) Impaired long distance functional connectivity and weighted network architecture in Alzheimer's disease. *Cereb Cortex* **24**, 1422-1435.

[44] He Y, Wang L, Zang Y, Tian L, Zhang X, Li K, Jiang T (2007) Regional coherence changes in the early stages of Alzheimer's disease: A combined structural and resting-state functional MRI study. *Neuroimage* **35**, 488-500.

[45] Oakes TR, Fox AS, Johnstone T, Chung MK, Kalin N, Davidson RJ (2007) Integrating VBM into the General Linear Model with voxelwise anatomical covariates. *Neuroimage* **34**, 500-508.

[46] Ashburner J, Friston KJ (2000) Voxel-based morphometry–the methods. *Neuroimage* **11**, 805-821.

[47] Thomas JB, Brier MR, Bateman RJ, Snyder AZ, Benzinger TL, Xiong C, Raichle M, Holtzman DM, Sperling RA, Mayeux R, Ghetti B, Ringman JM, Salloway S, McDade E, Rossor MN, Ourselin S, Schofield PR, Masters CL, Martins RN, Weiner MW, Thompson PM, Fox NC, Koeppe RA, Jack CR Jr, Mathis CA, Oliver A, Blazey TM, Moulder K, Buckles V, Hornbeck R, Chhatwal J, Schultz AP, Goate AM, Fagan AM, Cairns NJ, Marcus DS, Morris JC, Ances BM (2014) Functional connectivity in autosomal dominant and late-onset Alzheimer disease. *JAMA Neurol* **71**, 1111-1122.

[48] López L, Sanjuán MAF (6) (2002) Relation between structure and size in social networks. *Phys Rev E Stat Nonlin Soft Matter Phys* **65**(3 Pt 2A), 036107.

[49] Jiang T, He Y, Zang Y, Weng X (2004) Modulation of functional connectivity during the resting state and the motor task. *Hum Brain Mapp* **22**, 63-71.

[50] Golay X, Kollias S, Stoll G, Meier D, Valavanis A, Boesiger P (1998) A new correlation-based fuzzy logic clustering algorithm for fMRI. *Magn Reson Med* **40**, 249-260.

[51] Power JD, Barnes KA, Snyder AZ, Schlaggar BL, Petersen SE (2012) Spurious but systematic correlations in functional connectivity MRI networks arise from subject motion. *Neuroimage* **59**, 2142-2154.

[52] Satterthwaite TD, Wolf DH, Loughead J, Ruparel K, Elliott MA, Hakonarson H, Gur RC, Gur RE (2012) Impact of in-scanner head motion on multiple measures of functional connectivity: Relevance for studies of neurodevelopment in youth. *Neuroimage* **60**, 623-632.

[53] Van Dijk KR, Sabuncu MR, Buckner RL (2012) The influence of head motion on intrinsic functional connectivity MRI. *Neuroimage* **59**, 431-438.

[54] Yan CG, Cheung B, Kelly C, Colcombe S, Craddock RC, Di Martino A, Li Q, Zuo XN, Castellanos FX, Milham MP (2013) A comprehensive assessment of regional variation in the impact of head micromovements on functional connectomics. *Neuroimage* **76**, 183-201.

[55] Montembeault M, Rouleau I, Provost JS, Brambati SM, Alzheimer's Disease Neuroimaging Initiative (2015) Altered gray matter structural covariance networks in early stages of Alzheimer's disease. *Cereb Cortex*, doi: 10.1093/cercor/bhv105

[56] Buckner RL, Andrews-Hanna JR, Schacter DL (2008) The brain's default network: Anatomy, function, and relevance to disease. *Ann N Y Acad Sci* **1124**, 1-38.

[57] Andrews-Hanna JR, Reidler JS, Huang C, Buckner RL (2010) Evidence for the default network's role in spontaneous cognition. *J Neurophysiol* **104**, 322-335.

[58] Andrews-Hanna JR, Smallwood J, Spreng RN (2014) The default network and self-generated thought: Component processes, dynamic control, and clinical relevance. *Ann N Y Acad Sci* **1316**, 29-52.

[59] Buckner RL, Sepulcre J, Talukdar T, Krienen FM, Liu H, Hedden T, Andrews-Hanna JR, Sperling RA, Johnson KA (2009) Cortical hubs revealed by intrinsic functional connectivity: Mapping, assessment of stability, and relation to Alzheimer's disease. *J Neurosci* **29**, 1860-1873.

[60] Lehmann M, Madison CM, Ghosh PM, Seeley WW, Mormino E, Greicius MD, Gorno-Tempini ML, Kramer JH, Miller BL, Jagust WJ, Rabinovici GD (2013) Intrinsic connectivity networks in healthy subjects explain clinical variability in Alzheimer's disease. *Proc Natl Acad Sci U S A* **110**, 11606-11611.

[61] Seeley WW, Menon V, Schatzberg AF, Keller J, Glover GH, Kenna H, Reiss AL, Greicius MD (2007) Dissociable intrinsic connectivity networks for salience processing and executive control. *J Neurosci* **27**, 2349-2356.

[62] Menon V (2013) Developmental pathways to functional brain networks: Emerging principles. *Trends Cogn Sci* **17**, 627-640.

[63] Sridharan D, Levitin DJ, Menon V (2008) A critical role for the right fronto-insular cortex in switching between central-executive and default-mode networks. *Proc Natl Acad Sci U S A* **105**, 12569-12574.

[64] Insel PS, Mattsson N, Donohue MC, Mackin RS, Aisen PS, Jack CR Jr, Shaw LM, Trojanowski JQ, Weiner MW (2015) Alzheimer's Disease Neuroimaging, Initiative. The transitional association between beta-amyloid pathology and regional brain atrophy. *Alzheimers Dement* **11**, 1171-1179.

[65] Dai Z, Yan C, Li K, Wang Z, Wang J, Cao M, Lin Q, Shu N, Xia M, Bi Y, He Y (2015) Identifying and mapping connectivity patterns of brain network hubs in Alzheimer's disease. *Cereb Cortex* **25**, 3723-3742.

[66] Cai S, Huang L, Zou J, Jing L, Zhai B, Ji G, von Deneen KM, Ren J, Ren A, Alzheimer's Disease Neuroimaging, Initiatiave (2015) Changes in thalamic connectivity in the early and late stages of amnestic mild cognitive impairment: A resting-state functional magnetic resonance study from ADNI. *PLoS One* **10**, e0115573.

[67] Lewis DA, Campbell MJ, Terry RD, Morrison JH (1987) Laminar and regional distributions of neurofibrillary tangles and neuritic plaques in Alzheimer's disease: A quantitative study of visual and auditory cortices. *J Neurosci* **7**, 1799-1808.

[68] Morrison JH, Hof PR, Bouras C (1991) An anatomic substrate for visual disconnection in Alzheimer's disease. *Ann N Y Acad Sci* **640**, 36-43.

[69] Nyberg L, Petersson KM, Nilsson LG, Sandblom J, Aberg C, Ingvar M (2001) Reactivation of motor brain areas during explicit memory for actions. *Neuroimage* **14**, 521-528.

[70] Russ MO, Mack W, Grama CR, Lanfermann H, Knopf M (2003) Enactment effect in memory: Evidence concerning the function of the supramarginal gyrus. *Exp Brain Res* **149**, 497-504.

[71] Dubois B, Feldman HH, Jacova C, Hampel H, Molinuevo JL, Blennow K, DeKosky ST, Gauthier S, Selkoe D, Bateman R, Cappa S, Crutch S, Engelborghs S, Frisoni GB, Fox NC, Galasko D, Habert MO, Jicha GA, Nordberg A, Pasquier F, Rabinovici G, Robert P, Rowe C, Salloway S, Sarazin M, Epelbaum S, de Souza LC, Vellas B, Visser PJ, Schneider L, Stern Y, Scheltens P, Cummings JL (2014) Advancing research diagnostic criteria for Alzheimer's disease: The IWG-2 criteria. *Lancet Neurol* **13**, 614-629.

[72] Dubois B, Feldman HH, Jacova C, Dekosky ST, Barberger-Gateau P, Cummings J, Delacourte A, Galasko D, Gauthier S, Jicha G, Meguro K, O'Brien J, Pasquier F, Robert P, Rossor M, Salloway S, Stern Y, Visser PJ, Scheltens P (2007) Research criteria for the diagnosis of Alzheimer's disease: Revising the NINCDS-ADRDA criteria. *Lancet Neurol* **6**, 734-746.

[73] Liang X, Zou Q, He Y, Yang Y (2016) Topologically reorganized connectivity architecture of default-mode, executive-control, and salience networks across working memory task loads. *Cereb Cortex* **26**, 1501-1511.

[74] Delbeuck X, Collette F, Van der Linden M (2007) Is Alzheimer's disease a disconnection syndrome? Evidence from a crossmodal audio-visual illusory experiment. *Neuropsychologia* **45**, 3315-3323.

[75] Delbeuck X, Van der Linden M, Collette F (2003) Alzheimer's disease as a disconnection syndrome. *Neuropsychol Rev* **13**, 79-92.

[76] He X, Qin W, Liu Y, Zhang X, Duan Y, Song J, Li K, Jiang T, Yu C (2014) Abnormal salience network in normal aging and in amnestic mild cognitive impairment and Alzheimer's disease. *Hum Brain Mapp* **35**, 3446-3464.

[77] Long X, Zhang L, Liao W, Jiang C, Qiu B (2013) Alzheimer's Disease Neuroimaging, Initiative Distinct laterality alterations distinguish mild cognitive impairment and Alzheimer's disease from healthy aging: Statistical parametric mapping with high resolution MRI. *Hum Brain Mapp* **34**, 3400-3410.

[78] Song J, Qin W, Liu Y, Duan Y, Liu J, He X, Li K, Zhang X, Jiang T, Yu C (2013) Aberrant functional organization within and between resting-state networks in AD. *PLoS One* **8**, e63727.

[79] Brier MR, Thomas JB, Ances BM (2014) Network dysfunction in Alzheimer's disease: Refining the disconnection hypothesis. *Brain Connect* **4**, 299-311.

[80] Zhou J, Gennatas ED, Kramer JH, Miller BL, Seeley WW (2012) Predicting regional neurodegeneration from the healthy brain functional connectome. *Neuron* **73**, 1216-1227.

[81] Jilka SR, Scott G, Ham T, Pickering A, Bonnelle V, Braga RM, Leech R, Sharp DJ (2014) Damage to the salience network and interactions with the default mode network. *J Neurosci* **34**, 10798-10807.

[82] Chiong W, Wilson SM, D'Esposito M, Kayser AS, Grossman SN, Poorzand P, Seeley WW, Miller BL, Rankin KP (2013) The salience network causally influences default mode network activity during moral reasoning. *Brain* **136**, 1929-1941.

[83] Zhou J, Seeley WW (2014) Network dysfunction in Alzheimer's disease and frontotemporal dementia: Implications for psychiatry. *Biol Psychiatry* **75**, 565-573.

[84] Uddin LQ, Supekar K, Lynch CJ, Khouzam A, Phillips J, Feinstein C, Ryali S, Menon V (2013) Salience network-based classification and prediction of symptom severity in children with autism. *JAMA Psychiatry* **70**, 869-879.

[85] Grady CL, McIntosh AR, Beig S, Keightley ML, Burian H, Black SE (2003) Evidence from functional neuroimaging of a compensatory prefrontal network in Alzheimer's disease. *J Neurosci* **23**, 986-993.

[86] Dickerson BC, Salat DH, Greve DN, Chua EF, Rand-Giovannetti E, Rentz DM, Bertram L, Mullin K, Tanzi RE, Blacker D, Albert MS, Sperling RA (2005) Increased hippocampal activation in mild cognitive impairment compared to normal aging and AD. *Neurology* **65**, 404-411.

[87] Qi Z, Wu X, Wang Z, Zhang N, Dong H, Yao L, Li K (2010) Impairment and compensation coexist in amnestic MCI default mode network. *Neuroimage* **50**, 48-55.

[88] Agosta F, Pievani M, Geroldi C, Copetti M, Frisoni GB, Filippi M (2012) Resting state fMRI in Alzheimer's disease: Beyond the default mode network. *Neurobiol Aging* **33**, 1564-1578.

[89] Wang Z, Xia M, Dai Z, Liang X, Song H, He Y, Li K (2015) Differentially disrupted functional connectivity of the subregions of the inferior parietal lobule in Alzheimer's disease. *Brain Struct Funct* **220**, 745-762.

[90] Fox MD, Snyder AZ, Vincent JL, Corbetta M, Van Essen DC, Raichle ME (2005) The human brain is intrinsically

organized into dynamic, anticorrelated functional networks. *Proc Natl Acad Sci U S A* **102**, 9673-9678.

[91] Thompson WH, Fransson P (2015) The frequency dimension of fMRI dynamic connectivity: Network connectivity, functional hubs and integration in the resting brain. *Neuroimage* **121**, 227-242.

[92] Murphy K, Bodurka J, Bandettini PA (2007) How long to scan? The relationship between fMRI temporal signal to noise ratio and necessary scan duration. *Neuroimage* **34**, 565-574.